25th ABCM International Congress of Mechanical Engineering
October 20-25, 2019, Uberlândia, MG, Brazil

COBEM2019-1950
METHOD FOR CONSIDERING THE REAL AREA MOMENT OF INERTIA IN BENDING TESTS OF EXTRUDED PLA PARTS WITH DIFFERENT INFILL PERCENTAGES

Igor Cesar de Carlos Rosa[1]
Giannini Barcellos de Oliveira[2]
Arthur Alves Fiocchi[3]
Universidade Federal de Uberlândia. Av. João Naves de Ávila 2121, Câmpus Santa Mônica, CEP 38408-100, Uberlândia, Brazil.
[1]igor_cesarcr@hotmail.com, [2]giannini-jm2@hotmail.com, [3]arthurfiocchi@ufu.br

Abstract. *The Additive Manufacturing (AM) techniques have an increasing demand in the industry and in academia. This is mainly because lighter, stronger, and even more complex shapes are difficult or impossible to be produced by traditional machining techniques, known as Subtractive Manufacturing (SM). The AM has been gaining prominence by combining the fabrication of objects and functional assembled sets of complex macro geometries up until now difficult to be fabricated in a single step by associating different materials and properties. The present work aims to study the mechanical properties of extruded PLA workpieces by means of three-point bending tests and proposes a new method for determining the Ultimate Flexural Stress (UFS) considering the workpiece infill percentages (P). The bending tests were adapted from the ASTM D790 standard and considered the real area moment of inertia of the workpieces having different percentage of hexagonal (H) infills, P = 0 %, 10 %, 20 %, and 30%. The proposed method provided different mechanical strength from those obtained by ASTM D790. The percentage increase of the UFS was inversely proportional to the increase of the material infill percentage. One of the intentions of this paper is to draw attention to the lack of specific standards to evaluate the mechanical properties of parts fabricated by AM mainly with controlled internal voids. Future specific technical standards for static and dynamic testing of parts produced by AM must take into account outer and inner geometry of parts with infill percentage of less than 100 %.*

Keywords: *Additive Manufacturing; 3D printing; FDM; Three-Point Bending Test; Area Moment of Inertia.*

1. INTRODUCTION

The end of the industrial protection on Stratasys's patented 3D printing technology of polymer extrusion named Fused Deposition Modeling (FDM) in 2014 led to a rapid increase in the production of machines and services with a reduction in price of 3D printers and raw materials (Coon et al., 2016). The late entry of this manufacturing method limited the studies performed in this field and consequently did not elucidate the influence of all process parameters on the mechanical strength of printed parts. Many process parameters influences have not yet been analyzed scientifically, and many of the results already presented cannot be applied to different materials, geometric sets and AM methods and techniques. At the moment there are still many uncertainties regarding the mechanical static and mainly dynamic, behavior of parts produced by FDM (Singh et al., 2017; Brian et al., 2014).

The AM by extrusion of polymeric material is capable of building parts layer by layer from a wide range of thermoplastic materials typically in the form of filaments, such as Acrylonitrile Butadiene Styrene (ABS), Polycarbonate (PC), Polycarbonate Acrylonitrile Butadiene Styrene (PC-ABS), Polylactic Acid (PLA), Polyether Ether-Ketone (PEEK), Polyetherimide (PEI) (Bourell et al., 2017), Thermoplastic Polyurethane (TPU), Polyphenylsulfone (PPSU) (Singh et al., 2017) and Nylon (Singh et al., 2015; Bourell et al., 2017). Among these thermoplastics, the PLA is characterized by the lowest average melting temperature (Chacon et al., 2017), respectable mechanical properties, good surface finish as well as it is biodegradability and biocompatibility (Drumright et al., 2000; Franco et al., 2016).

One of the main advantages of some AM technologies is the possibility of varying infill geometry and percentage of material into the 3D printed object. However, no specific standard for determining the mechanical strength of parts manufactured by AM with less than 100 % infill was found in literature. ASTM D790-17 – "*Flexural Properties of Unreinforced and Reinforced Plastics and Electrical Insulating Materials*" is one of the standards used to determine the properties of plastic parts made by AM. On the other hand, despite of providing guidance on machine and apparatus configurations, minimum number of tests and approximate external geometry and dimensions of workpieces, ASTM D790-17 does not establish any criterion (order or quantity) of the production of the parts or methods of stress analysis for workpieces with interior not fully filled.

This research proposes a new method for determining the mechanical properties by means of a three-point bending test of parts made by AM with nonhomogeneous interior, comparing the results with ASTM D790-17. The results presented and discussed in this research are incipient and are just a fraction of a larger research about the influences of the materials and input parameters on mechanical performance of parts additively manufactured.

2. EXPRIMENTAL SETUP

In this study a three-axis Cartesian CL2 Pro^{+} polymeric extrusion 3D printer with enclosure, heated table, and blue filaments with 1.75 mm diameter, both supplied by the Brazilian company Cliever®, were used. The mechanical properties of the Cliever blue PLA were not provided by the manufacturer. The choice of the blue color is due to the characteristics of the material that favor its observation in optical microscope compared to all the other tested colors. In order to avoid thermal, physical or chemical influences of the raw PLA prior to the AM, two rolls of 1 kg PLA filaments of the same production batch were used, which were sealed and stored together in dark and dry environment.

The workpieces were modeled in the SolidWorks® CAD software according to the dimensions recommended by ASTM D790-17, it means 127.0 mm length, 12.7 mm width, and 3.2 mm thickness for three-point bending test. Then the STL 3D models were exported to the Cliever Studio® software to be converted to .CL format, specific to the Cliever® 3D printer. The 3D printing parameters defined for evaluating the influence of the infill percentage (P) on the mechanical strength are shown in Table 1. The parameters of the extrusion process were selected according to literature review, research group experience, and the 3D printer features with the objective to achieve light and mechanically resistant pats without critical defects. Some examples are delamination, localized lack of material, distortion, and out of dimensional tolerance, which could negatively influence performance of the workpieces in the three-point bending tests.

Table 1. Additive manufacturing process parameters for extruded PLA.

Variable Parameters	Infill percentage (P)	0 %; 10 %; 20 %; 30 %
Fixed Parameters	Nozzle diameter	0.35 mm
	Raster strategy	Hexagonal (H)
	Build orientation	Flat
	Infill orientation	45°
	Quantity of perimeter layers	2
	Quantity of bottom and top layers	2 and 2
	Extrusion temperature	185 °C
	Table temperature (first and other layers)	40 °C and 50 °C
	Layer thickness	0.19 mm
	Distance between workpieces during printing process	3.0 mm
	Filament color	Blue Cliever®
	3D printer	Cliever CL2 Pro^{+}®

Following the recommendation of the ASTM D790-17, five workpieces having the same input process parameters were submitted to the three-point bending tests to determine their mechanical properties for each maximum load (F). After printing, the workpieces were packed in PVC bags and hermetically sealed to minimize absorption of moisture and influence of light. The bags were stored in dark and dry environment. The WPs were only removed from their package during mass and dimension measurements and bending tests. All workpieces had the same life time between printing and bending tests, and were always handled wearing talc-free nitrile gloves.

The bending tests were performed on MTS Landmark® 647 universal test machine with feed rate of 1.3653 mm/min and 51 mm distance between clamp supports, in accordance with ASTM D790-17. The bending tests lasted until the load reached its maximum value.

2.1 UFS for real area moment of inertia

The recommended ASTM D790-17 equation for determining the three-point ultimate flexural strength (UFS) (Equation 1) is not indicated to be applied for parts having an infill percentage lower than 100 % due to the area moment of inertia (I) [m^4] is based on a solid rectangular cross-section b.h [mm^2] with no pores or any other type of voids. Hence, the cross-section must be completely dense according to ASTM D790-17.

$$\mathrm{UFS} = \frac{3\mathrm{FL}}{2\mathrm{bh}^2} \tag{1}$$

where F is the load at the moment of rupture [N], L the distance between beam supports [m], b width [m], and h height of the workpiece [m].

The Equation 1 can be mathematically represented by the division between the product of the bending moment (M) [N.m] and distance to neutral line (y) [m] by I (Equation 2).

$$UFS = \frac{M \cdot y}{I} \tag{2}$$

Considering the rectangular section of sides b and h massive, I can be expressed by Equation 3.

$$I = \int_{\frac{-b}{2}}^{\frac{b}{2}} \left(\int_{\frac{-h}{2}}^{\frac{h}{2}} y^2 \cdot dy \right) dx = \frac{bh^3}{12} \tag{3}$$

However, by varying the infill percentage and geometry, among other 3D printing parameters such as contour quantity, base and top thicknesses, deposited filament geometry, interfilamentous porosity etc., real area moment of inertia (I_{real}) cannot be simplified by the external dimensions b and h section of the workpiece such as in ASTM D790-17. Thus, the area differential (dA) in the Cartesian plane XY of the cross-section with the load F applied in the Y direction must be taken into account.

In this work, the numerical value of the I_{real} was calculated by means of the ideal CAD model of the parts which were modeled in SolidWorks® from the STL files considering the adopted extrusion parameters shown in Table 2. The I_{real} was calculated by solving, therefore, the Equation 3 for which cross-section.

The boundary conditions of the proposed model take for granted that the workpiece cross-section under the greatest mechanical stress is also under maximum bending moment (M_{max}). The values of the external dimensions of the workpieces were defined as the measured dimensions acquired during the experiments, that is, the printed parts have dimensional deviations that were taking into account. According to Camargo (2019) the typical quality index of extruded PLA ranges from IT10 to IT14.

It was assumed that the thickness of the first printed layer was equal to the others and the thickness and width of the deposited filament equal to 0.45 mm and 0.19 mm, respectively. Interfaces between layers were assumed to have the same properties of the whole workpiece. The external measurements of width, thickness, and length represented the arithmetic mean among all the workpieces of the set.

The dimensions of the workpieces were measured using a Mitutoyo 530-312B-10 caliper with resolution of 0.01 mm. Twenty measurements were taken for each workpiece; ten for the thickness and ten for the width. Measurements were taken in distributed way throughout the workpiece to properly represent the geometry of the piece with one dimension for each axis.

The design of the workpieces made in Solid Works® followed the steps shown in flow chart presented in Fig. 1. It was made one design for each set of workpieces manufactured with the same input parameters. The external and contour dimensions were chosen as equal to the average measurements of all workpieces in a set made of the same input parameters.

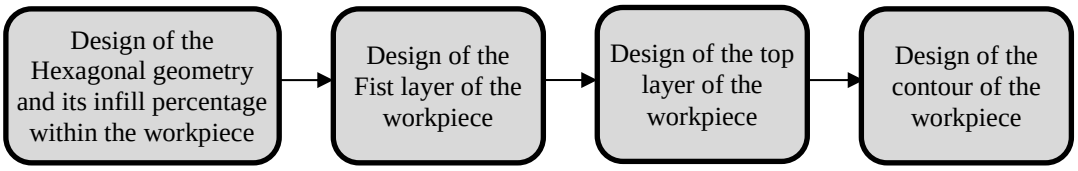

Figure 1. Steps taken to design the workpieces' CAD models with the real dimensions in Solid Works®.

The design geometry of the workpieces considered only the intentionally implemented infill, disregarding possible pores, voids or any deposition failures among deposited filaments. Thus, the calculated moment of inertia is likely to be greater than the actual moment of inertia of the printed workpieces.

The percentage difference between UFS_{real} (proposed method) and $UFS_{apparent}$ (according to the ASTM D790-17) was calculated using Equation 4:

$$\left(\frac{UFS_{real} - UFS_{apparent}}{UFS_{real}} \right) x\, 100\% \tag{4}$$

The masses of the workpieces were determined using an analytical scale OHAUS®, model AS120S with 0.0001 g resolution. Each workpiece's mass was measured five times on the same day of the bending test, the final mass of each set considered all five measurements of every workpiece in the group. Evaluation of masses, dimensions, and bending tests happened in 20 ºC ambient temperature.

3. RESULTS AND DISCUSSION

Figure 2 presents a comparison of the workpieces' cross-sections (a) designed in SolidWorks® and (b) printed workpieces. The upper region of each workpiece was in contact with the moving cylinder. The photos indicate an influence of the manufacturing parameters in the porosity. These porosities appear to be increased proportionately with the increase of infill percentage. A difference in geometry between designed and printed parts is also shown. The proposed initial model did not considered de quasi cylindrical or elliptical shape of the deposited material that may introduce interfilamentar porosity, thus reducing the real cross-section area e introducing stress concentration.

A gradual change in coloration of the fractured workpieces can be seen in Fig. 2, ranging from blue (top) to white (bottom). These changes happened in the lower regions of the workpieces and were not symmetrically distribute throughout the body. The white regions have a similar texture that is encountered in fractured metal parts that fails with a fragile mode.

Bending test introduces two types of stresses into the workpiece, compression above neutral line and tensile bellow neutral line. The greatest compression and tensile stresses occur in the upper and lower parts of the workpiece, respectively. The gradual color variation may be related to stress fields into the workpieces during bending tests. It is noticed that 3D printed parts present non-homogenous stress distribution.

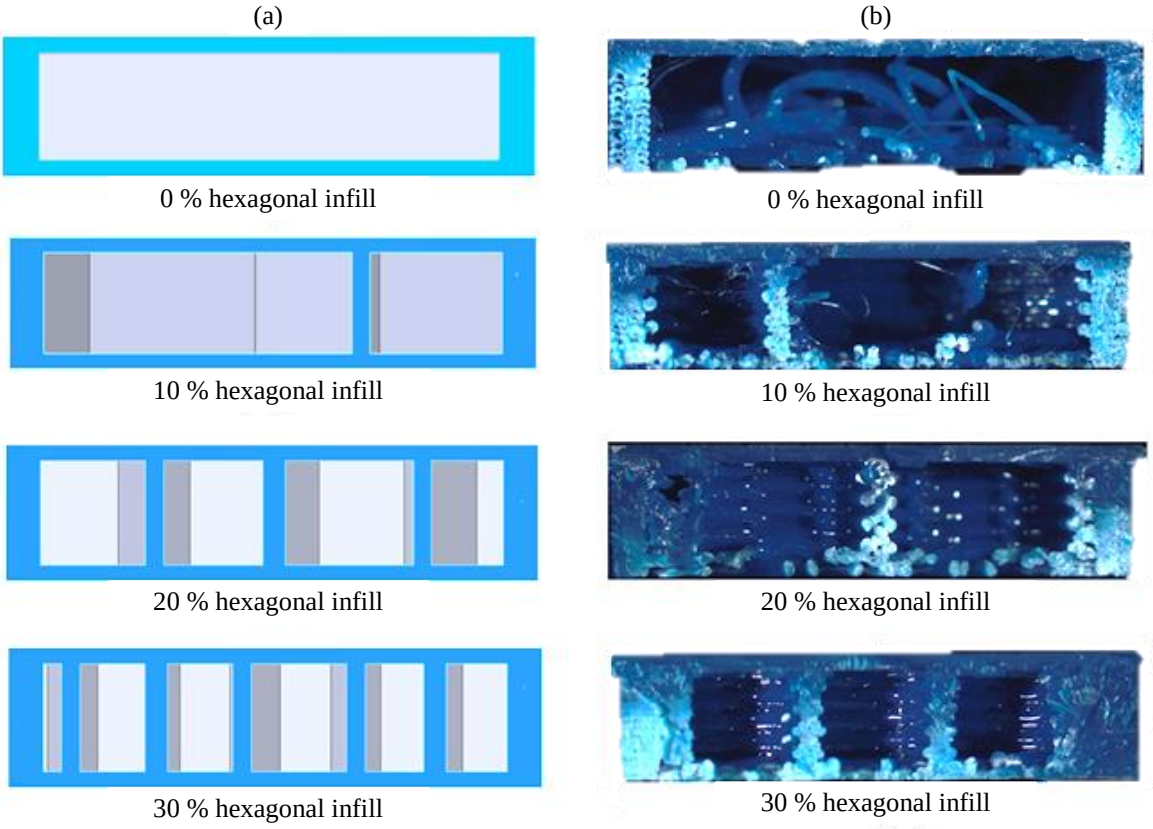

Figure 2 – Comparison between cross-sections of (a) CAD models and (b) real printed workpieces

Due to the lack of support material and distance between the walls as well as non-desired PLA extrusion, the lower the infill percentage, the higher the presence of non-intentional filament inside the hexagonal cavities. Those non-desired depositions are well exemplified for 0 % and 10 % hexagonal infill images shown in Fig. 2 (b). It is also revealed in Fig. 2 that increasing infill decreases porosity, and the real cross-section (b) approaches the theoretical one (a).

The pores and gaps presented within the workpieces should be more analyzed in future works, and these irregularities are influenced by extrusion process parameters.

Some workpieces showed an incomplete failure after reaching the maximum force. This particular behavior occurred in all workpieces with 0 % infill and, sporadically, in others with different infill percentages. This abrupt decrease in strength was derivate from the failure of the lower region of the workpiece that was under higher tensile stress. The subsequent resistance was due to some layers of the upper region that did not fracture, thus the cross-section area decreased drastically, so as the load supported by the workpiece. The test ended after the force reached its maximum value in order to avoid any possible damage to the machine.

UFS values calculated by Equation 2 considering the solid cross-section ($I_{apparent}$) according to ASTM D790-17 and by analyzing the I_{real} as a function of F proposed in this work are presented in Fig. 3.

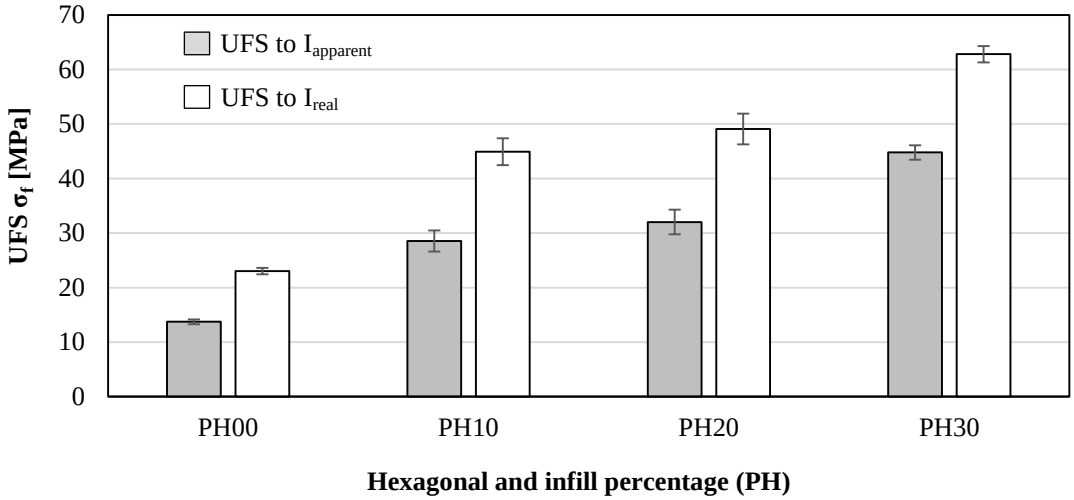

Figure 3. Ultimate flexural stress (UFS) of the Cliever's blue PLA as a function of infill percentage (P) and hexagonal raster (H) using apparent ($I_{apparent}$) and real (I_{real}) area moment of inertia.

A difference of up to 40 % in UFS was identified in the unfilled workpieces (PH00). The UFS difference was higher for those with lower infill percentage. Workpieces with 10 % infill (PH10) showed a difference of 36 % in UFS. Workpieces PH20 presented a change of 34 %. The highest UFS values were reached with PH30 and the difference between the UFS considering $I_{aparrent}$ and I_{real} was the lowest of all tested conditions, which was 28 %. Preliminary results suggest the larger the cross-sectional area, the closer $I_{apparent}$ to I_{real} is. When reaching full infill, the rectangular section will be massive and area b·h will be that assumed by ASTM D790-17. The values of the percentage differences between UFSs are shown in Table 2.

Using the data in Table 2, a third-degree polynomial (Equation 6) of the relative area moment of inertia (I_r) [%] was calculated as a function of the mass of the workpieces (m) [g]. The coefficient of determination (R^2) of Equation 5 is equal to one.

$$I_r = -2.9604m^3 + 28.794m^2 - 95.57m + 144.58 \quad (6)$$

Table 2 Percentage difference of ultimate flexural strength (UFS) between the real area moment of inertia (I_{real}) and apparent area moment of inertia ($I_{apparent}$) for different hexagonal infill percentages.

WP	Percentage difference between UFS [%]	Final mass [g]
PH00	40.3	2.3794
PH10	36.5	3.2492
PH20	34.8	3.8008
PH30	28.7	4.4448

4. CONCLUSION

The present research considered the real area moment of inertia (I) of extruded PLA workpieces to propose a new method for calculating Ultimate Flexural Strength (UFS) of parts not fully dense made by additive manufacturing (AM). One of the intentions of this paper is to draw attention to the lack of specific standards to evaluate the mechanical properties of parts fabricated by AM mainly with controlled internal voids. There are many AM methods and their process parameters have strong influence in performance of printed parts.

Results showed a significant difference between the values of UFS_{real} and $UFS_{apparent}$ when the real area moment of inertia is considered. These modifications are responsible for the approximation of the results of mechanical strength of workpieces with low and high infill density. The results also point out that the differences in strength between workpieces with high and low density infills are not as significant as indicated by the literature considering ASTM D790-17.

The percentage increase of the UFS was inversely proportional to the increase of the infill percentage. Future specific technical standards for mechanical testing of parts produced by AM must take into account geometry and area of the actual cross-section of parts with infill percentage of less than 100 %. The need for detailed standardization for parts made by AM is, therefore, necessary due to process parameters influence the mechanical strength.

This article is by no means intended to end the discussion of the theoretical determination of the mechanical strength of parts manufactured by AM, but rather to bring to light the importance of AM and its achievable benefits by favoring design of mechanical parts with higher performance.

5. REFERENCES

ASTM D790-17 ”Standard Test Methods for Flexural Properties of Unreinforced and Reinforced Plastics and Electrical Insulating Materials”. *ASTM International, West Conshohocken*, PA, 2017, https://doi.org/10.1520/D0790-17.

Brian, N. T., Robert, S. and Scoot, A. G., 2014. ”A review of melt extrusion additive manufacturing processes: I. Process design and modeling”. *Rapid Prototyping Journal*, Vol. 20 Issue: 3, pp. 192–204.

Bourell, D., Kruth, J. P., Leu, M., Levy, G., Rosen, D., Beese, A. M. and Clare, A., 2017. ”Materials for additive manufacturing”. *Manufacturing Technology,* Vol. 66, pp. 659–681.

Camargo, C. J., 2019. ”Estudo das propriedades mecâniccas, elétricas, tribológicas e de qualidade de peças manufaturadas pelo processo FDM utilizando os polímeros PLA-Grafeno e ABS-Condutivo” Thesys (Mechanical Engineering PhD) – Faculdade de Engenharia Mecânica, Universidade Federal de Uberlândia, Uberlândia.

Coon, C., Pretzel, B. and Lomax, T., 2016. ”Preserving rapid prototypes: a review”. Heritage science, Vol. 4, Chapter 40. https://doi.org/10.1186/s40494-016-0097-y.

Drumright, R. E., Gruber, P. R. and Henton, D. E., 2000. ”Polylactic Acid Technology”, *Advanced.Materials*. Vol. 12, N° 23.

Chacon, J. M., Caminero, M. A., Plaza, E. G. and Nunez, P. J., 2017 ”Additive manufacturing of PLA structures using fused deposition modelling: Effect of process parameters on mechanical properties and their optimal selection”. *Materials and design*, Vol. 124, pp. 143–157.

Franco, F.I., Auras, R., Burgess, G., Holmes, D., Fang, X., Rubino, M. and Soto-Valdez, H., 2016. “Concurrent solvent induced crystallization and hydrolytic degradation of PLA by water-ethanol solutions”. *Polymer*, Vol. 99, pp. 315–323.

Singh, S., Ramakrishna, S. and Singh, R., 2017. ”Material issues in additive manufacturing: A review”. *Journal of Manufacturing Processes*, Vol. 25, pp. 185–200.

Singh, R., Singh, J. and Singh S., 2015. ”Investigation for dimensional accuracy of AMC prepared by FDM assisted investment casting using nylon-6 waste based reinforced filament”. *Procedia Materials Science*, Vol. 6, pp. 851–858.

6. RESPONSIBILITY NOTICE

The authors are the only responsible for the printed material included in this paper.